Current status of V_{cb} project of LANL-SWME Collaboration

Weonjong Lee
(LANL-SWME Collaboration)

Lattice Gauge Theory Research Center,
Department of Physics and Astronomy, Seoul National University

April 9, MITP Workshop

Lattice fermion action

- **Sea quarks**: HISQ action with $N_f = 2 + 1 + 1$ dynamical flavors. The following ensembles are generated by the MILC collaboration.

ID	a (fm)	Volume	m'_ℓ/m'_s	$M_\pi L$	M_π (MeV)
a12m310	0.12	$24^3 \times 64$	1/5	4.54	305.3(4)
$a12m220$	0.12	$32^3 \times 64$	1/10	4.29	216.9(2)
$a12m130$	0.12	$48^3 \times 64$	1/27	3.88	131.7(1)
$a09m310$	0.09	$32^3 \times 96$	1/5	4.50	312.7(6)
$a09m220$	0.09	$48^3 \times 96$	1/10	4.71	220.3(2)
$a09m130$	0.09	$64^3 \times 96$	1/27	3.66	128.2(1)
⋮			⋮		

- **Valence light quarks** (u, d, s): HISQ action
- **Valence heavy quarks** (c, b): Oktay-Kronfeld action

Limitation of Fermilab action calculation → OK action

- Using the OK action, we expect the improvement in charm quark discretization error from the current Fermilab-MILC results of $h_{A_1}(w = 1)$, semileptonic form factor for $\bar{B} \to D^* \ell \bar{\nu}$ at zero recoil.

	$h_{A_1}(w = 1)$
source	error (%)
statistics	0.4
matching	0.4
χPT	0.5
$g_{D^* D_\pi}$	0.3
c discretization	$1.0 \to (0.2)_{\text{OK}}$
others	0.1
total	$1.4 \to (0.8)_{\text{OK}}$

- Belle II starts running fully on Dec. 2018 and the target statistics is 50 times larger than the previous Belle experiment.

Status

ID	κ_{crit}	κ_b, κ_c	3pt production	Excited state analysis
a12m310	○	○	○	△
$a12m220$	△			
$a12m130$				
$a09m310$	○	○	△	△
$a09m220$	○	○	△	
$a09m130$				
⋮			⋮	

- ○: Finished
- △: In progress

$\bar{B} \to D^* \ell \bar{\nu}$ at zero recoil: $h_{A_1}(1)$ and R

- $h_{A_1}(1)$: semileptonic form factor for $\bar{B} \to D^* \ell \bar{\nu}$ at zero recoil,

$$|h_{A_1}(1)|^2 = \frac{\langle D^* | A^j_{cb} | \bar{B} \rangle \langle \bar{B} | A^j_{bc} | D^* \rangle}{\langle D^* | V^4_{cc} | D^* \rangle \langle \bar{B} | V^4_{bb} | \bar{B} \rangle} \qquad \leftarrow \text{continuum formula}$$

[Fermilab-MILC, PRD79, 014506 (2009)]

- On the lattice, we calculate the double ratio R:

$$R(t, t_f) \equiv \frac{C^{B \to D^*}_{A_1}(t, t_f) C^{D^* \to B}_{A_1}(t, t_f)}{C^{B \to B}_{V_4}(t, t_f) C^{D^* \to D^*}_{V_4}(t, t_f)} \xrightarrow[t \to \infty]{t_f \to \infty} \left| \frac{h_{A_1}(1)}{\rho_{A_j}} \right|^2 \xrightarrow[a \to 0]{V \to \infty} |h_{A_1}(1)|^2$$

- $C^{X \to Y}_J(t, t_f)$: Lattice 3-point correlation functions
- ρ_{A_j}: Matching factor

3-point correlation function: current improvement

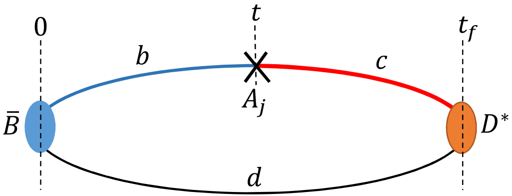

$$O_B = \bar{\psi}_b \gamma_5 \psi_d$$
$$O_{D^*} = \bar{\psi}_c \gamma_j \psi_d$$
$$A_j^{cb} = \bar{\Psi}_c \gamma_j \gamma_5 \Psi_b,$$

Current operator using the improved field $\Psi(x)$: [Leem, Lattice 2017]

$$\Psi(x) = e^{M_1/2}\Big[1 + d_1 \boldsymbol{\gamma}\cdot\boldsymbol{D} \qquad \rightarrow \mathcal{O}(\lambda^1)$$
$$+ d_2\Delta^{(3)} + d_B i\boldsymbol{\Sigma}\cdot\boldsymbol{B} + d_E \boldsymbol{\alpha}\cdot\boldsymbol{E} \qquad \rightarrow \mathcal{O}(\lambda^2)$$
$$+ d_{rE}\{\boldsymbol{\gamma}\cdot\boldsymbol{D}, \boldsymbol{\alpha}\cdot\boldsymbol{E}\} + d_3\sum_i \gamma_i D_i \Delta_i + d_4\{\boldsymbol{\gamma}\cdot\boldsymbol{D}, \Delta^{(3)}\}$$
$$+ d_5\{\boldsymbol{\gamma}\cdot\boldsymbol{D}, i\boldsymbol{\Sigma}\cdot\boldsymbol{B}\} + d_{EE}\{\gamma_4 D_4, \boldsymbol{\alpha}\cdot\boldsymbol{E}\} \qquad \rightarrow \mathcal{O}(\lambda^3)$$
$$+ d_6[\gamma_4 D_4, \Delta^{(3)}] + d_7[\gamma_4 D_4, i\boldsymbol{\Sigma}\cdot\boldsymbol{B}]\Big]\psi(x).$$

B-meson $2+2$ excited states

(Diagonal fit)

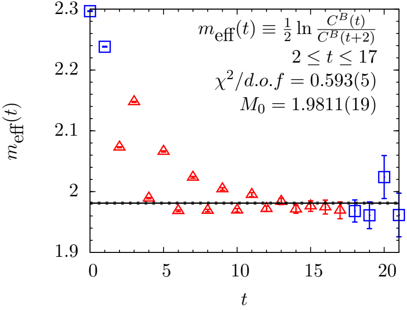

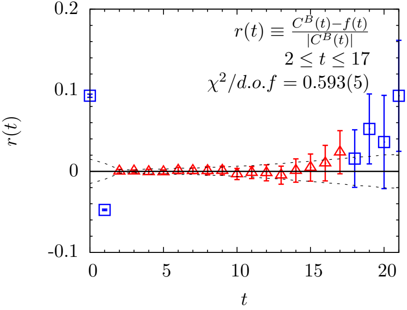

$$f(t) = g(t) + g(T-t)$$
$$g(t) = \mathcal{A}_0^2 e^{-M_0 t} + \mathcal{A}_2^2 e^{-M_2 t} - (-1)^t \mathcal{A}_1^2 e^{-M_1 t} - (-1)^t \mathcal{A}_3^2 e^{-M_3 t}$$

B- & D^*-meson $2+2$ excited states

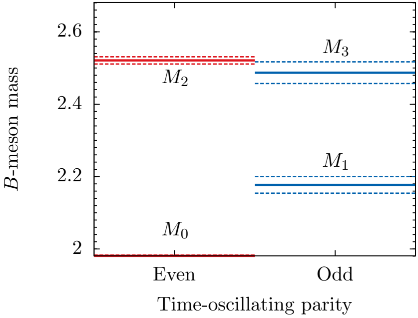

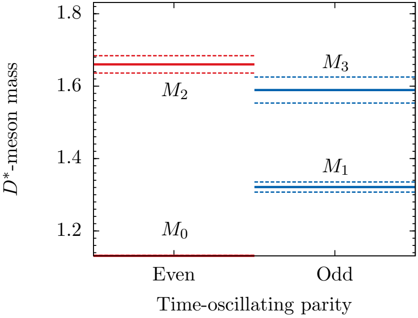

$\mathcal{A}_0^2 \cdot 10^{-2}$	1.498(27)
$\mathcal{A}_2^2/\mathcal{A}_0^2$	2.47(4)
$\mathcal{A}_1^2/\mathcal{A}_0^2$	0.51(13)
$\mathcal{A}_3^2/\mathcal{A}_0^2$	1.12(11)

$\mathcal{A}_0^2 \cdot 10^{-2}$	1.706(23)
$\mathcal{A}_2^2/\mathcal{A}_0^2$	2.24(16)
$\mathcal{A}_1^2/\mathcal{A}_0^2$	0.35(6)
$\mathcal{A}_3^2/\mathcal{A}_0^2$	1.22(11)

Excited state analysis on $C_J^{X\to Y}(t,t_f)$

$$
\begin{aligned}
C_{A_j}^{B\to D^*}(t,t_f) &= \langle O_{D^*}^\dagger(t_f) A_j^{cb}(t) O_B(0)\rangle \qquad (t_f > t > 0) \\
&= \mathcal{A}_0^{D^*}\mathcal{A}_0^{B}\langle D_0^*|A_j^{cb}|B_0\rangle e^{-M_{D_0^*}(t_f-t)} e^{-M_{B_0}t} \\
&\quad + \mathcal{A}_0^{D^*}\mathcal{A}_1^{B}\langle D_0^*|A_j^{cb}|B_1\rangle (-1)^t e^{-M_{D_0^*}(t_f-t)} e^{-M_{B_1}t} \\
&\quad + \mathcal{A}_1^{D^*}\mathcal{A}_0^{B}\langle D_1^*|A_j^{cb}|B_0\rangle (-1)^{t_f-t} e^{-M_{D_1^*}(t_f-t)} e^{-M_{B_0}t} \\
&\quad + \mathcal{A}_1^{D^*}\mathcal{A}_1^{B}\langle D_1^*|A_j^{cb}|B_1\rangle (-1)^{t_f} e^{-M_{D_1^*}(t_f-t)} e^{-M_{B_1}t} \\
&\quad + \mathcal{A}_2^{D^*}\mathcal{A}_0^{B}\langle D_2^*|A_j^{cb}|B_0\rangle e^{-M_{D_2^*}(t_f-t)} e^{-M_{B_0}t} \\
&\quad + \mathcal{A}_0^{D^*}\mathcal{A}_2^{B}\langle D_0^*|A_j^{cb}|B_2\rangle e^{-M_{D_0^*}(t_f-t)} e^{-M_{B_2}t} \\
&\quad + (\cdots)
\end{aligned}
$$

To achieve the sub-percent precision calculation, we have to be able to control the excited state contamination.

Excited state analysis on $C_J^{X\to Y}(t,t_f)$

- We generated 3pt functions $C_J^{X\to Y}(t,t_f)$ for six source-sink separations $t_f = 10,\ 11,\ 12,\ 13,\ 14,\ 15$.
- We found consistent simultaneous fit results using various choice of t_f set and so far, the best fit is taken from the set $t_f = 10,\ 11,\ 12,\ 13$.
- We include $n, m = 0, 1, 2$ states for $|B_m\rangle$ and $|D^*_n\rangle$.
- We set the fit parameters $\langle B_1|V^4_{bb}|B_0\rangle$, $\langle D^*_1|V^4_{cc}|D^*_0\rangle$, $\langle D^*_1|A^j_{cb}|B_0\rangle$, $\langle D^*_0|A^j_{cb}|B_1\rangle$ to zero because the fitting results are consistent with zero for them.

Excited state analysis on $C_J^{X\to Y}(t, t_f)$

- $\langle B|V^4_{bb}|B\rangle$: $C^{B\to B}_{V_4}(t, t_f)$ simultaneous fit
  - 2 fit parameters: $\langle B_0|V^4_{bb}|B_0\rangle$, $\langle B_1|V^4_{bb}|B_1\rangle$.
- $\langle D^*|V^4_{cc}|D^*\rangle$: $C^{D^*\to D^*}_{V_4}(t, t_f)$ simultaneous fit
  - 2 fit parameters: $\langle D^*_0|V^4_{cc}|D^*_0\rangle$, $\langle D^*_1|V^4_{cc}|D^*_1\rangle$.
- $\langle D^*|A^j_{cb}|B\rangle$: $C^{B\to D^*}_{A_1}(t, t_f)$ and $C^{D^*\to B}_{A_1}(t, t_f)$ simultaneous fit
  - 7 fit parameters: $\langle D^*_0|A^j_{cb}|B_0\rangle$, $\langle D^*_1|A^j_{cb}|B_1\rangle$, $\langle D^*_2|A^j_{cb}|B_0\rangle$, $\langle D^*_0|A^j_{cb}|B_2\rangle$, $\langle D^*_2|A^j_{cb}|B_1\rangle$, $\langle D^*_1|A^j_{cb}|B_2\rangle$ and $\langle D^*_2|A^j_{cb}|B_2\rangle$,

$C_{V_4}^{B\to B}(t, t_f)$ simultaneous fit

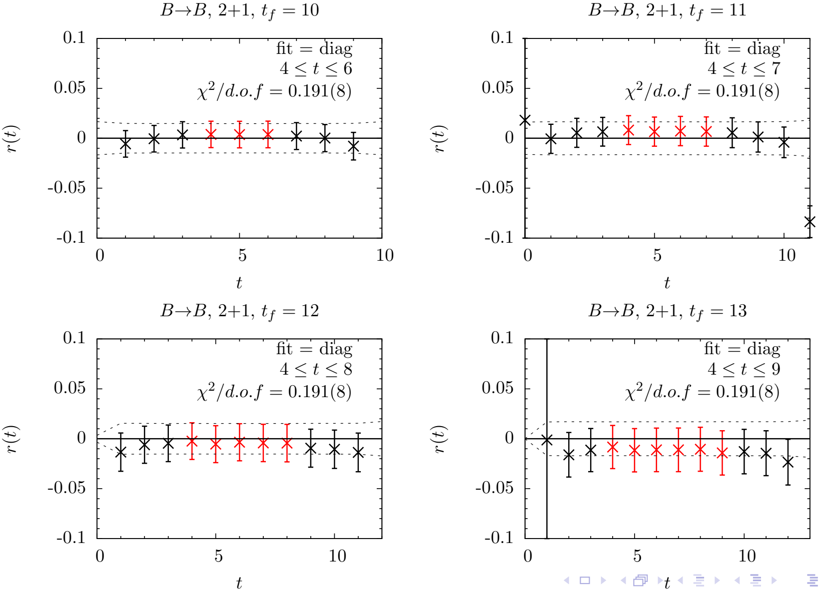

$C_{V_4}^{D^*\to D^*}(t,t_f)$ simultaneous fit

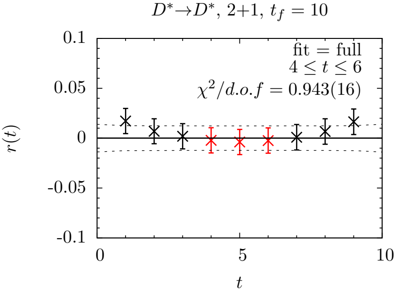

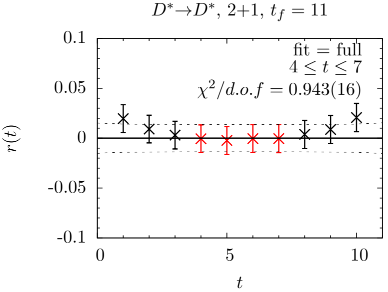

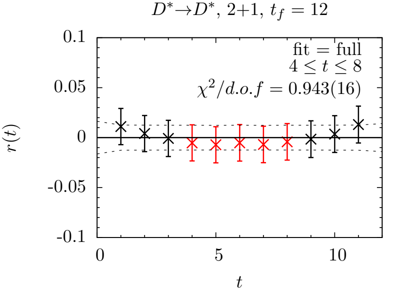

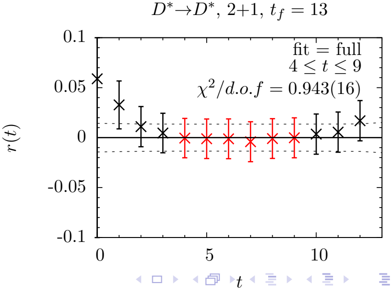

$C_{A_1}^{B\to D^*}(t,t_f)$ & $C_{A_1}^{D^*\to B}(t,t_f)$ simultaneous fit

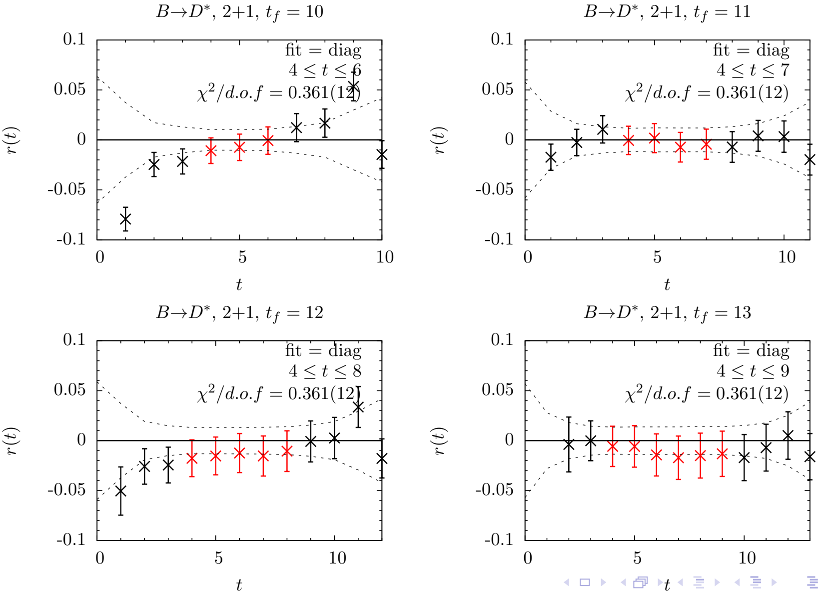

$C_{A_1}^{B\to D^*}(t,t_f)$ & $C_{A_1}^{D^*\to B}(t,t_f)$ simultaneous fit

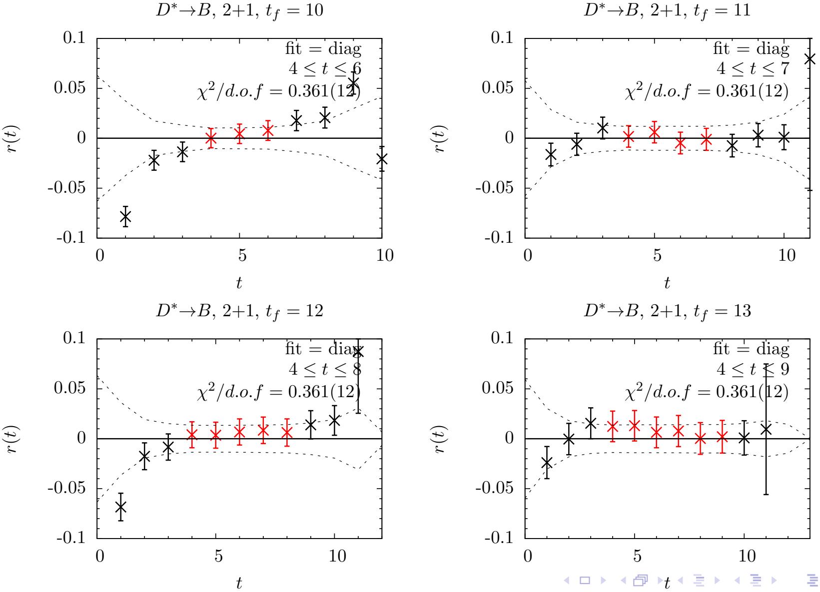

Very preliminary results on $\sqrt{R} = |h_{A_1}(1)/\rho_{A_j}|$

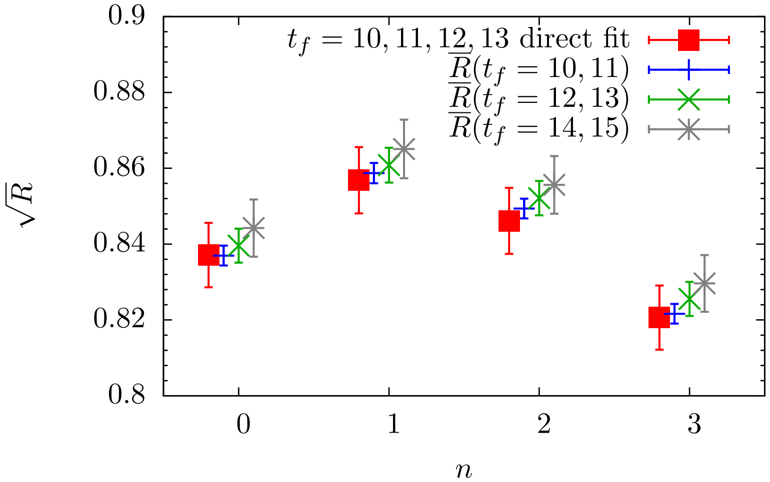

- n: the order of the current improvement.
- $\overline{R}(t, t_f) \equiv \frac{1}{2}R(t, t_f) + \frac{1}{4}R(t, t_f + 1) + \frac{1}{4}R(t + 1, t_f + 1)$

Summary

- We produced V_{cb} related 3-point correlation functions (for $\bar{B} \to D^{(*)}\ell\bar{\nu}$).
- We obtained preliminary result of $\dfrac{h_{A_1}(1)}{\rho_{A_j}}$, $\bar{B} \to D^{*}\ell\bar{\nu}$ semileptonic form factor at zero recoil. We cannot quote any number because the analysis is preliminary, yet.
- This is the first numerical study of the hadronic matrix element using the Oktay-Kronfeld action with current operators improved up to $\mathcal{O}(\lambda^3)$.

To be done

- Perturbative calculation of ρ_{A_j}
- Extending measurement to fine, superfine, and ultrafine ensembles.
- Chiral-continuum extrapolation